Inorg. Chem. **2005**, *44*, 2367–2375

Mechanistic Insights from Reactions between Copper(II)–Phenoxyl Complexes and Substrates with Activated C–H Bonds

Russell C. Pratt and T. Daniel P. Stack*

Department of Chemistry, Stanford University, Stanford, California 94305

Received September 16, 2004

The reactivities of two copper(II)–phenoxyl analogues of the oxidized, active form of the metalloenzyme galactose oxidase, [**1**^{tBu2}]$^+$ and [**2**^{tBu2}]$^+$, have been studied using the substrates benzyl alcohol and 9,10-dihydroanthracene, for a total of four reactions. The reaction stoichiometries in all cases show a 2:1 ratio of oxidant to benzaldehyde or anthracene product, indicating that [**1**^{tBu2}]$^+$ and [**2**^{tBu2}]$^+$ behave ultimately as only one-electron oxidants, but the reaction kinetics each indicate that only a single copper(II)–phenoxyl complex is involved in the rate-determining step. For each substrate, rate laws indicate that [**1**^{tBu2}]$^+$ and [**2**^{tBu2}]$^+$ react by different mechanisms: one proceeds by a simple bimolecular reaction, while the other first enters into a substrate-binding equilibrium before subsequently reacting by an intramolecular reaction. The reactions proceeding by the latter mechanism have faster overall rates, which correlates to a lower entropic barrier for the substrate-binding mechanism. Correlation of the reaction rates with the C–H bond dissociation energies of substrates as well as significant deuterium kinetic isotope effects indicates that the rate-determining steps involve hydrogen atom abstraction from the activated C–H bonds. A variable-temperature study (268–308 K) of the nonclassical KIE of the [**1**^{tBu2}]$^+$/benzyl alcohol reaction ($k_H/k_D = 15$ at 298 K) failed to show evidence for quantum tunneling. The rapid sequence by which a second 1 equiv of copper(II)–phenoxyl oxidant completes the reaction after the rate- and product-determining hydrogen atom abstraction step cannot be probed kinetically. Comparisons are made to the reactivities of other copper(II)–phenoxyl complexes reported in the literature and to galactose oxidase itself.

Introduction

The enzyme galactose oxidase (GOase) catalyzes the aerobic oxidation of primary alcohols to aldehydes.[1−3] Key to its function are its two one-electron cofactors in its active site, a single copper atom and a cysteine-modified tyrosine residue, that act cooperatively to accomplish two-electron substrate-oxidizing and dioxygen-reducing half-reactions in a "ping-pong" type mechanism. Starting from the enzyme in its fully oxidized copper(II)−tyrosine radical state, the essential steps of alcohol oxidation appear to be binding of alcohol to copper and deprotonation by a nearby tyrosine residue, abstraction of the α-C−H atom by the tyrosine radical, and single electron transfer from the substrate to the enzyme (Figure 1). Reactivity studies have probed the reaction profile of the substrate-oxidizing half-reaction, with further corroboration from computational studies.[4,5] The hydrogen atom abstraction and electron transfer steps have not been kinetically distinguished, and the events may be in fact indistinguishable.[6]

GOase's intriguing use of both inorganic and organic cofactors has inspired both modeling efforts intended to study its reactivity and a more general investigation of metal−phenoxyl complexes.[7,8] Stoichiometric reactions are observed between metal−phenoxyl complexes and alcohols or other substrates.[9−16] The use of small molecules allows facile characterization of the reaction kinetics, and the reaction

* Author to whom correspondence should be addressed. E-mail: stack@stanford.edu.

(1) Whittaker, J. W. *Chem. Rev.* **2003**, *103*, 2347−2363.
(2) Whittaker, J. W.; Whittaker, M. M. *Pure Appl. Chem.* **1998**, *70*, 903−910.
(3) Klinman, J. P. *Chem. Rev.* **1996**, *96*, 2541−2562.
(4) Wachter, R. M.; Branchaud, B. P. *Biochim. Biophys. Acta* **1998**, *1384*, 43−54.
(5) Himo, F.; Eriksson, L. A.; Maseras, F.; Siegbahn, P. E. M. *J. Am. Chem. Soc.* **2000**, *122*, 8031−8036.
(6) Whittaker, M. M.; Whittaker, J. W. *Biochemistry* **2001**, *40*, 7140−7148.
(7) Jazdzewski, B. A.; Tolman, W. B. *Coord. Chem. Rev.* **2000**, *200*, 633−685.
(8) Itoh, S.; Taki, M.; Fukuzumi, S. *Coord. Chem. Rev.* **2000**, *198*, 3−20.
(9) Chaudhuri, P.; Hess, M.; Florke, U.; Wieghardt, K. *Angew. Chem., Int. Ed.* **1998**, *37*, 2217−2220.
(10) Chaudhuri, P.; Hess, M.; Weyhermüller, T.; Wieghardt, K. *Angew. Chem., Int. Ed.* **1999**, *38*, 1095−1098.
(11) Chaudhuri, P.; Hess, M.; Müller, J.; Hildenbrand, K.; Bill, E.; Weyhermüller, T.; Wieghardt, K. *J. Am. Chem. Soc.* **1999**, *121*, 9599−9610.

10.1021/ic048695i CCC: $30.25
Published on Web 02/23/2005

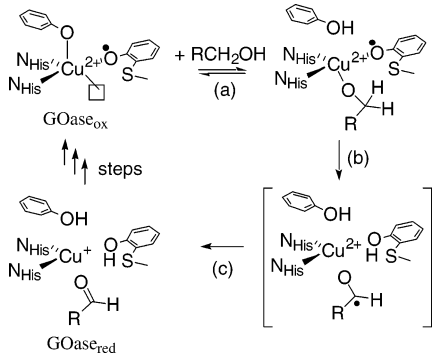

Figure 1. Consensus mechanism for the substrate-oxidizing half-reaction of GOase. Steps: (a) binding of alcoholic substrate to the exchangeable equatorial position on copper with simultaneous proton transfer to the axial tyrosine; (b) hydrogen atom abstraction from substrate by the equatorial tyrosine radical to form a transiently stable ketyl intermediate; (c) reduction of the enzyme by electron transfer from the ketyl to copper and formation of an aldehyde product.

pathways are generally found to involve hydrogen atom abstraction as is proposed for GOase. Copper(II)−phenoxyl complexes in particular are usually found to accomplish two-electron oxidations by using the oxidizing equivalents resulting from both the copper(II)/copper(I) and phenoxyl/phenolate redox couples.[12,15,16] In the presence of air and generally under basic conditions, some of these well-defined copper(II)−phenoxyl complexes can catalyze the aerobic oxidation of alcohols in biomimetic fashion.[10,15,17] Recently reported alcohol oxidation catalysts based on copper ions and other organic cofactors such as azodicarboxylates or nitroxyl radicals also imitate GOase's use of mixed cofactors, though it is unclear whether the inorganic and organic cofactors work cooperatively in the same manner in these systems.[18,19]

Our work has turned to focus on derivatives of the copper(II)−phenolate complexes $\mathbf{1}^{tBu2}$ and $\mathbf{2}^{tBu2}$ (Chart 1).[20] These complexes are very similar structurally, but the phenolates of $\mathbf{2}^{tBu2}$ are more easily oxidized and more basic than those in $\mathbf{1}^{tBu2}$ due to the reduction of the imine moieties. Upon ligand-centered oxidation under radical-stabilizing conditions, these complexes form monocationic, copper(II)−phenoxyl derivatives ($[\mathbf{1}^{tBu2}]^+$ and $[\mathbf{2}^{tBu2}]^+ = [Cu^{II}L^{\bullet}]^+$) that constitute analogues of the fully oxidized form of GOase. Furthermore, $[\mathbf{1}^{tBu2}]^+$ and $[\mathbf{2}^{tBu2}]^+$ react with the model substrate benzyl

Chart 1

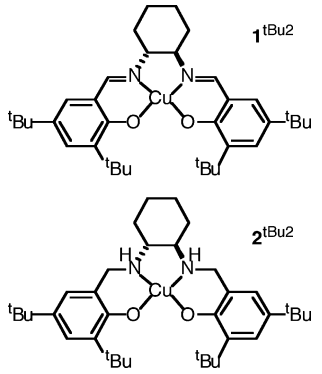

Scheme 1

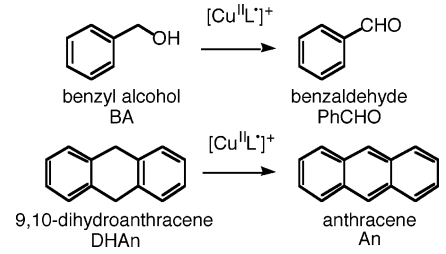

alcohol to produce benzaldehyde and thereby mimic the substrate-oxidizing half-reaction of GOase (Scheme 1). Initial studies of the reactions of $[\mathbf{1}^{tBu2}]^+$ and $[\mathbf{2}^{tBu2}]^+$ with benzyl alcohol quickly established several interesting points. Though $[\mathbf{2}^{tBu2}]^+$ is a significantly weaker oxidant than $[\mathbf{1}^{tBu2}]^+$ (CH_2Cl_2: $\Delta(E^{\circ\prime}) = 370$ mV),[20] it reacts ∼10 times faster with benzyl alcohol as a substrate at room temperature. The accelerated reaction rate appears to arise from mechanistic differences between the two reactions, for while the reaction of $[\mathbf{1}^{tBu2}]^+$ with benzyl alcohol follows a second-order rate law implying a simple bimolecular reaction, the reaction of $[\mathbf{2}^{tBu2}]^+$ shows saturation behavior at high substrate concentrations. This observation suggests that a substrate-binding equilibrium occurs prior to a committed reaction step, which would be analogous to substrate-binding steps observed for many enzymes, including GOase. Also, the reactions of both $[\mathbf{1}^{tBu2}]^+$ and $[\mathbf{2}^{tBu2}]^+$ with benzyl-d_2 alcohol demonstrated nonclassical kinetic isotope effects, which are rarely observed among reactive GOase model compounds.

In light of these results, we wished to extend the study of the reactivities of $[\mathbf{1}^{tBu2}]^+$ and $[\mathbf{2}^{tBu2}]^+$. To better characterize the reactions of $[\mathbf{1}^{tBu2}]^+$ and $[\mathbf{2}^{tBu2}]^+$ with benzyl alcohol, the activation parameters for their rate-determining steps have been determined by kinetic analysis at multiple temperatures. By studying the enthalpic and entropic contributions to the free energies of activation, we hoped to understand both the relative hydrogen atom abstraction abilities of the two copper(II)−phenoxyl complexes and the contribution of the substrate-binding equilibrium to the more rapid reaction rate of $[\mathbf{2}^{tBu2}]^+$. Variable-temperature studies have also been used to search for experimental evidence of quantum tunneling effects in the reaction of $[\mathbf{1}^{tBu2}]^+$ with benzyl alcohol. In addition, the reactions of $[\mathbf{1}^{tBu2}]^+$ and $[\mathbf{2}^{tBu2}]^+$ with the benchmark hydrogen atom abstraction substrate 9,10-dihy-

(12) Itoh, S.; Taki, M.; Takayama, S.; Nagatomo, S.; Kitagawa, T.; Sakurada, N.; Arakawa, R.; Fukuzumi, S. *Angew. Chem., Int. Ed.* **1999**, *38*, 2774−2776.
(13) Taki, M.; Kumei, H.; Itoh, S.; Fukuzumi, S. *J. Inorg. Biochem.* **2000**, *78*, 1−5.
(14) Itoh, S.; Kumei, H.; Nagatomo, S. K., T.; Fukuzumi, S. *J. Am. Chem. Soc.* **2001**, *123*, 2165−2175.
(15) Thomas, F.; Gellon, G.; Gautier-Luneau, I.; Saint-Aman, E.; Pierre, J.-L. *Angew. Chem., Int. Ed.* **2002**, *41*, 3047−3050.
(16) Sénèque, O.; Campion, M.; Douziech, B.; Giorgi, M.; Le Mest, Y.; Reinaud, O. *Dalton Trans.* **2003**, 4216−4218.
(17) Wang, Y.; DuBois, J. L.; Hedman, B.; Hodgson, K. O.; Stack, T. D. P. *Science* **1998**, *279*, 537−540.
(18) Markó, I. E.; Gautier, A.; Dumeunier, R. L.; Doda, K.; Phillipart, F.; Brown, S. M.; Urch, C. J. *Angew. Chem., Int. Ed.* **2004**, *43*, 1588−1591.
(19) Gamez, P.; Arends, I. W. C. E.; Reedjik, J.; Sheldon, R. A. *Chem. Commun.* **2003**, 2414−2415.
(20) Pratt, R. C.; Stack, T. D. P. *J. Am. Chem. Soc.* **2003**, *125*, 8716−8717.

droanthracene have been studied (Scheme 1). By using an alternate substrate, we hoped to channel the reactivities of $[\mathbf{1}^{tBu2}]^+$ and $[\mathbf{2}^{tBu2}]^+$ into a common mechanism and thereby facilitate comparisons.

Experimental Section

(a) Materials and Methods. Reagents and solvents were commercially available and used as received unless otherwise noted. Benzoyl chloride and benzaldehyde were of the highest available grade; benzaldehyde was stored under a N_2 atmosphere prior to use. Dihydroanthracene-9,9,10,10-d_4 was prepared by a literature procedure.[21] CH_2Cl_2 was distilled from P_2O_5 or CaH_2, and THF was distilled from Na/benzophenone; both solvents were stored under an atmosphere of dry N_2 prior to use. ^{1}H NMR spectra were obtained on a Varian XL-400 spectrometer operating at 400 MHz; all samples were dissolved in $CDCl_3$. Electronic (UV−vis−NIR) spectra were collected using a Polytec X-DAP spectrophotometer (190−820 nm) or a Cary 50 spectrophotometer (190−1100 nm) equipped with a custom fiber optic dip probe from Hellma, Inc. Tandem gas chromatography−mass spectrometry was performed using a Hewlett-Packard HP6890/5973 instrument.

(b) Syntheses. α-Benzyl-d_2 Alcohol. Under a N_2 atmosphere, to a chilled (0 °C), stirring suspension of lithium aluminum deuteride (98+% "D", 1 g, 26 mmol) in dry THF (50 mL) was added dropwise a solution of benzoyl chloride (5.9 g, 42 mmol) in THF (25 mL). When addition was completed, the solution was refluxed for 2 h and then cooled (0 °C) and quenched by dropwise addition of 10 mL of 1:1 (v/v) THF/H_2O. The resulting mixture was acidified with 100 mL 1 M aqueous HCl and then extracted with Et_2O (100 mL, then 2 × 20 mL). The combined organic fractions were washed with 10% (w/v) aqueous K_2CO_3 (50 mL) and saturated brine (50 mL) before being dried over solid anhydrous K_2CO_3, filtered, and evaporated to give 4.0 g of the title compound (90% yield). ^{1}H NMR: δ 7.4−7.3 (m, 5H, ArH), 1.83 (s, 1H, OH; varies with H_2O content); no CH_2 peak observed. GC-MS: *m*/*z* 110 (M^+). To ensure reproducibility of rate measurements, α-benzyl-d_2 alcohol was stirred with barium oxide and distilled in vacuo immediately prior to reactivity studies.

α-Benzyl-d_1 Alcohol. This substrate was synthesized by the same method used for α-benzyl-d_2 alcohol with minor changes: benzaldehyde (9.0 g, 85 mmol) and lithium aluminum deuteride (98+% "D", 1 g, 26 mmol) were used, and the solution was kept at 0 °C for the duration of the reaction. The yield of α-benzyl-d_1 alcohol was 9.0 g (98%). ^{1}H NMR: δ 7.4−7.3 (m, 5H, Ar*H*), 4.66 (dt, $^2J_{HD}$ = 1.8 Hz, $^3J_{HH}$ = 6.0 Hz, 1H, C*H*DOH), 1.96 (d, $^3J_{HH}$ = 6.0 Hz, 1H, O*H*). GC-MS: *m*/*z* 109 (M^+).

Acetylferrocenium Hexafluoroantimonate ($AcFc^+SbF_6^-$). Under dry N_2, a solution of $AgSbF_6$ (68 mg, 0.2 mmol) in 15 mL of Et_2O was added a solution of AcFc (46 mg, 0.2 mmol) in 5 mL of Et_2O, immediately upon which a green precipitate formed. After the solution was left to stand for 1 h, the precipitate was isolated by filtration. The solid was then suspended in 20 mL of CH_2Cl_2, rapidly forming a blue solution. This solution was filtered through a CH_2Cl_2-wetted plug of Celite to generate a deep blue, saturated solution of $AcFc^+SbF_6^-$ (∼7 mM). The volume needed to oxidize $\mathbf{2}^{tBu2}$ to $[\mathbf{2}^{tBu2}]^+$ was determined by spectrophotometric titration of CH_2Cl_2 solutions of $\mathbf{2}^{tBu2}$ of known concentration.

$[\mathbf{1}^{tBu2}]^+SbF_6^-$. To a solution of $\mathbf{1}^{tBu2}$ (15 mg, 25 μmol) in CH_2Cl_2 (1 mL) was added a solution of $AgSbF_6$ (8.5 mg, 25 μmol) in CH_2Cl_2 (1 mL). The resulting purple solution was filtered through a CH_2Cl_2-wetted plug of Celite and the volume made up to 5.0 mL to generate a 5 mM solution of $[\mathbf{1}^{tBu2}]^+SbF_6^-$ that was stable and usable for weeks.

(c) Rate Measurements. The solution of substrate (0.05−1.0 M) in CH_2Cl_2 (10 mL) was sealed under N_2 in a custom reaction cell and adjusted to the appropriate reaction temperature. Reactions with $[\mathbf{1}^{tBu2}]^+$ were initiated by adding 200 μL of a 5 mM solution of $[\mathbf{1}^{tBu2}]^+SbF_6^-$ in CH_2Cl_2. Reactions with $[\mathbf{2}^{tBu2}]^+$ were initiated by first adding 200 μL of a 5 mM solution of $\mathbf{2}^{tBu2}$ in CH_2Cl_2 and then adding ∼160 μL of a ∼7 mM solution of $AcFc^+SbF_6^-$. Absorbance spectra were then obtained over the range 320−800 nm for approximately 5 half-lives. Due to its fast rate, the $[\mathbf{1}^{tBu2}]^+$/DHAn reaction was monitored at a single wavelength (557 nm). Kinetic analyses for most reactions were performed by multiwavelength fitting of the spectra using the commercial program Specfit/32.

(d) Product Analyses of Intramolecular KIEs. A 200 μL volume of 5 mM $[\mathbf{1}^{tBu2}]^+SbF_6^-$ or $\mathbf{2}^{tBu2}$ was adjusted to the desired reaction temperature, and then 1 μL (∼1 mg, 10 μmol, 10 eq) of α-benzyl-d_1 alcohol was added, followed by ∼160 μL of ∼7 mM $AcFc^+SbF_6^-$ to the $\mathbf{2}^{tBu2}$ solution. The vials were then sealed and left to stand for what was estimated to be 5 half-lives, from 1 day at 308 K to 2 weeks at 268 K. The reaction solutions were then analyzed directly by tandem GC-MS. Mass spectra of genuine samples of benzaldehyde-*h* and -*d* have distinct intensity patterns of the *m*/*z* 105−108 peaks. The intensity pattern of the same peaks in the mass spectrum of the mixture of *h*- and *d*-benzaldehyde produced by reaction of $[\mathbf{1}^{tBu2}]^+$ or $[\mathbf{2}^{tBu2}]^+$ with α-benzyl-d_1 alcohol were fit as a linear least-squares fit of the individual benzaldehyde-*h* and -*d* intensity patterns.[22]

Results

(a) Reactions with Benzyl Alcohol. Solutions of purple $[\mathbf{1}^{tBu2}]^+$ or blue $[\mathbf{2}^{tBu2}]^+$ in CH_2Cl_2 (SbF_6^- counterion, 0.1 mM) are stable for days or hours, respectively. After addition of benzyl alcohol (0.10−1.0 M) to these solutions, the colors fade within minutes to faint greens. Gas chromatographic (GC) analysis of the final solutions shows that benzaldehyde is produced in up to a 1:2 ratio relative to the initial amount of phenoxyl complex. While most reactions were conducted under dioxygen-free conditions, the presence of air did not affect the benzaldehyde yields. UV−vis spectra of the final solutions show weak d−d absorptions in the visible region, indicating that the final copper product is in the +2 oxidation state, but the spectra do not match those of neutral $\mathbf{1}^{tBu2}$ or $\mathbf{2}^{tBu2}$. Addition of 1 equiv of base (NEt_3) to the final solutions does restore the UV−vis spectra to those of neutral $\mathbf{1}^{tBu2}$ or $\mathbf{2}^{tBu2}$, so the final copper-containing products appear to be protonated copper(II) complexes $[\mathbf{1}^{tBu2}H]^+$ and $[\mathbf{2}^{tBu2}H]^+$. Most likely, the abstracted proton is bonded to the oxygen atom of one of the ligating phenolates, resulting in copper(II)−phenol−phenolate species similar to those that have been structurally characterized.[15,23−25]

(21) Goldsmith, C. R.; Jonas, R. T.; Stack, T. D. P. *J. Am. Chem. Soc.* **2002**, *124*, 83−96.

(22) Kwart, H.; George, T. J. *J. Org. Chem.* **1979**, *44*, 162−164.

(23) Auerbach, U.; Eckert, U.; Wieghardt, K.; Nuber, B.; Weiss, J. *Inorg. Chem.* **1990**, *29*, 938−944.

(24) Sokolowski, A.; Leutbecher, H.; Weyhermüller, T.; Schnepf, R.; Both, E.; Bill, E.; Hildebrandt, P.; Wieghardt, K. *J. Biol. Inorg. Chem.* **1997**, *2*, 444−453.

(25) Shimazaki, Y.; Huth, S.; Odani, A.; Yamauchi, O. *Angew. Chem., Int. Ed.* **2000**, *39*, 1666−1669.

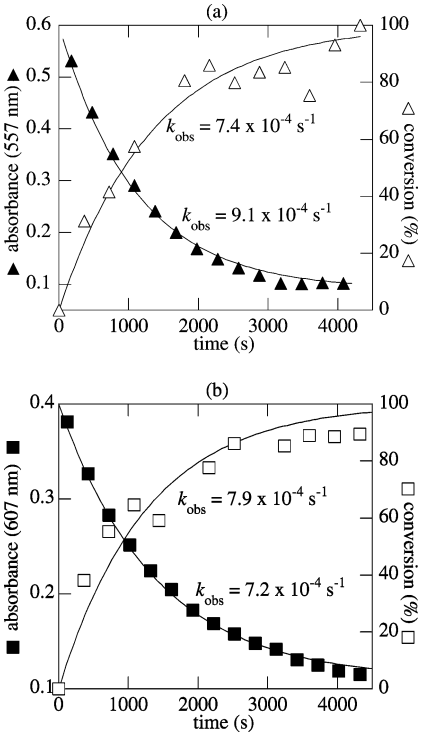

Figure 2. Correlation of UV−vis and GC data for benzyl alcohol oxidations: (a) decay in absorption at 557 nm (solid triangles) and benzaldehyde formation (open triangles) for the reaction of $[\mathbf{1}^{tBu2}]^+$ (0.1 mM) with 0.50 M benzyl alcohol, shown with exponential fits; (b) decay in absorption at 607 nm (solid squares) and benzaldehyde formation (open squares) for the reaction of $[\mathbf{2}^{tBu2}]^+$ (0.1 mM) with 0.050 M benzyl alcohol, shown with exponential fits. Agreement of the k_{obs} values is reasonable given the scatter in the GC data, which is a result of approaching the detection limit for benzaldehyde of the instrument.

The overall stoichiometry of the reaction observed is then

$$2[Cu^{II}L^{\bullet}]^+ + PhCH_2OH \rightarrow 2[Cu^{II}LH]^+ + PhCHO$$

The intense visible absorptions of $[\mathbf{1}^{tBu2}]^+$ and $[\mathbf{2}^{tBu2}]^+$ make their reactions with benzyl alcohol suitable for spectrophotometric studies to explore the rates, kinetics, and mechanism. Monitoring by UV−vis spectroscopy and GC analysis in both cases shows that the decay of the optical features is correlated to the appearance of benzaldehyde (Figure 2), confirming that reaction of $[Cu^{II}L^{\bullet}]^+$ leads directly to product formation. In the presence of excess benzyl alcohol (1000−10 000 equiv), the transformation of optical features from $[Cu^{II}L^{\bullet}]^+$ to $[Cu^{II}LH]^+$ is best fit as a pseudo-first-order process, $d[[Cu^{II}L^{\bullet}]^+]/dt = -k_{obs}[[Cu^{II}L^{\bullet}]^+]$, suggesting that only a single molecule of $[Cu^{II}L^{\bullet}]^+$ is involved in the rate-determining step for both complexes despite the overall involvement of two molecules of $[Cu^{II}L^{\bullet}]^+$ in the stoichiometry of the reaction. The first-order rate constants are unchanged when the initial concentations of $[Cu^{II}L^{\bullet}]^+$ are varied, further supporting unimolecular involvement. When the concentrations of benzyl alcohol are varied, though, the kinetic behaviors of the two reactions are found to diverge (Figure 3). For $[\mathbf{1}^{tBu2}]^+$, k_{obs} is linearly dependent on the benzyl alcohol concentration (0.10−1.0 M), giving an overall second-order rate expression $d[[\mathbf{1}^{tBu2}]^+]/dt = -k_2[[\mathbf{1}^{tBu2}]^+][PhCH_2OH]$ with

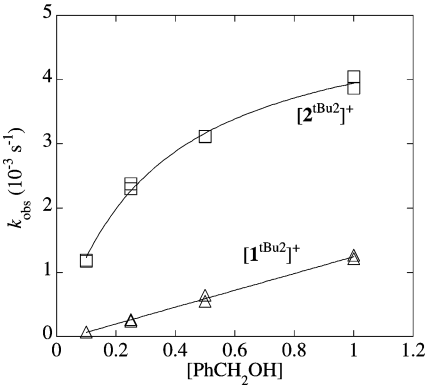

Figure 3. Concentration dependence of k_{obs} for the reactions of $[\mathbf{1}^{tBu2}]^+$ (triangles) and $[\mathbf{2}^{tBu2}]^+$ (squares) with benzyl alcohol at 25 °C. The data are shown with a linear fit for $[\mathbf{1}^{tBu2}]^+$ (slope = (1.31 ± 0.04) × 10^{-3} M^{-1} s^{-1}, intercept = (−0.07 ± 0.03) × 10^{-3} s^{-1}) and a saturated fit based on eq 1 for $[\mathbf{2}^{tBu2}]^+$ (k_1 = (5.23 ± 0.14) × 10^{-3} s^{-1}, K = 3.0 ± 0.2 M^{-1}).

$k_2 = (1.31 \pm 0.04) \times 10^{-3}$ M^{-1} s^{-1} at298 K. For $[\mathbf{2}^{tBu2}]^+$, the dependence of k_{obs} on substrate concentrations appears to saturate at high concentrations (Figure 3). The expression for k_{obs} for an associative mechanism in which a substrate-binding equilibrium precedes an intramolecular rate-determining step is given in eq 1

$$k_{obs} = \frac{k_1 K[PhCH_2OH]}{1 + K[PhCH_2OH]} \quad (1)$$

The rate data for $[\mathbf{2}^{tBu2}]^+$ are fit well to this equation, giving values of $k_1 = (5.23 \pm 0.14) \times 10^{-3}$ s^{-1} and $K = 3.0 \pm 0.2$ at 298 K. The equilibrium constant indicates that, over the benzyl alcohol concentration of 0.10−1.0 M, the fraction of $[\mathbf{2}^{tBu2}]^+$ associated with substrate varies substantially, from ∼20% to ∼75%; however, the UV−vis spectrum of $[\mathbf{2}^{tBu2}]^+$ in the reaction mixtures is unaffected. In anticipation that the interaction involves weak binding of an alcohol or alcoholate to the copper center in a GOase-like fashion, the potential competitive inhibitor 1-octanol was added to $[\mathbf{2}^{tBu2}]^+$−benzyl alcohol reaction mixtures. However, addition of up to 1.0 M 1-octanol had no substantial effect on the rate of reaction as monitored by the rate of decay of $[\mathbf{2}^{tBu2}]^+$. For both $[\mathbf{1}^{tBu2}]^+$ and $[\mathbf{2}^{tBu2}]^+$, slightly faster decay rates were observed when reactions were performed with unpurified CH_2Cl_2 or benzyl alcohol, most likely due to unproductive side reactions. Air had no effect on reaction rates.

To determine whether C−H bond cleavage is involved in the rate-determining steps of benzyl alcohol oxidation, the reaction rates of $[\mathbf{1}^{tBu2}]^+$ and $[\mathbf{2}^{tBu2}]^+$ with α-benzyl-d_2 alcohol were measured at 298 K. For $[\mathbf{1}^{tBu2}]^+$, the rate constant found at $[PhCD_2OH] = 1.0$ M is $k_2(D) = (6.62 \pm 0.35) \times 10^{-5}$ s^{-1}, representing a kinetic isotope effect of $k_2(H)/k_2(D) = 19$. For $[\mathbf{2}^{tBu2}]^+$, measurements of $k_{obs}(D)$ over a range of concentrations and analysis of $k_{obs}(D)$ with eq 1 gives values of $k_1(D) = (5.2 \pm 0.2) \times 10^{-4}$ s^{-1} and $K(D) = 3.9 \pm 0.6$ and KIEs of $k_1(H)/k_1(D) = 10$ and $K(H)/K(D) = 0.8$. Because the reactions are very slow, these reactions are highly sensitive to impurities; anomalous rates were observed if the α-benzyl-d_2 alcohol was not distilled immediately before use. The high KIE values could be confirmed by intra-

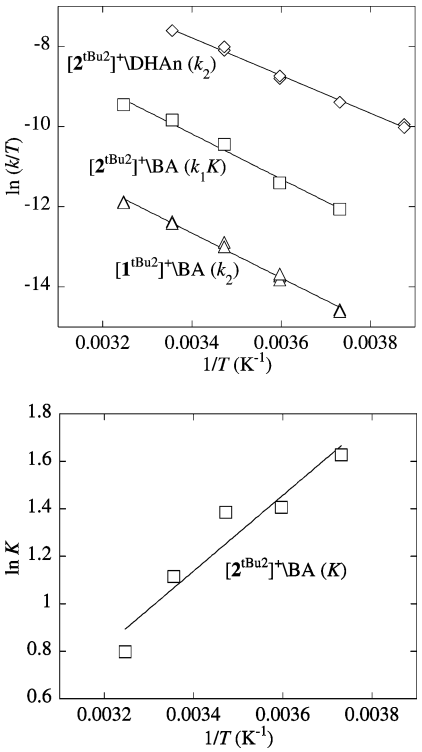

Figure 4. Top: Eyring analysis by linear fits of the temperature dependence of the rate constants k_2 and k_1K for the reactions of benzyl alcohol (BA) with $[\mathbf{1}^{tBu2}]^+$ (triangles; slope = −5600 ± 200 K, intercept = 6.4 ± 0.6) and $[\mathbf{2}^{tBu2}]^+$ (squares; slope = −5600 ± 400 K, intercept = 8.9 ± 1.3) and k_2 for the reaction of DHAn with $[\mathbf{2}^{tBu2}]^+$ (diamonds; slope = −4700 ± 100 K, intercept = 5.8 ± 0.4), over the range 258−308 K. Bottom: van't Hoff analysis of the temperature dependence of the BA/$[\mathbf{2}^{tBu2}]^+$ equilibrium constant K over the rage 268−308 K, shown with a linear fit (slope = 1600 ± 300 K, intercept = −4.3 ± 1.0).

molecular competition experiments with the labeled substrate α-benzyl-d_1 alcohol. GC-MS analysis of the reaction products allows for deconvolution of the distinct mass spectra of benzaldehyde-*h* and benzaldehyde-*d* resulting from *d*-abstraction and *h*-abstraction, respectively.[22] The intramolecular KIE values so determined for $[\mathbf{1}^{tBu2}]^+$ and $[\mathbf{2}^{tBu2}]^+$ are 15 and 11, respectively, uncorrected for secondary KIEs. This intramolecular experiment truly measures the isotope effect of the product-determining step of the reaction. However, given that the KIE results for the intermolecular and intramolecular experiments are similar, the rate-determining and product-determining steps appear to be identical for both reactions.

(b) Variable-Temperature Studies. To further study the difference between the reaction mechanisms of $[\mathbf{1}^{tBu2}]^+$ and $[\mathbf{2}^{tBu2}]^+$, the reaction rates were studied as a function of temperature (268−308 K) to extract the activation parameters. Rate constants for the $[\mathbf{1}^{tBu2}]^+$/benzyl alcohol and $[\mathbf{2}^{tBu2}]^+$/benzyl alcohol reactions at multiple temperatures are listed in the Supporting Information, and Eyring and van't Hoff analyses are pictured in Figure 4. For the $[\mathbf{1}^{tBu2}]^+$/benzyl alcohol reaction, the activation parameters are found to be $\Delta H^{\ddagger} = (11.1 \pm 0.4)$ kcal mol^{-1} and $\Delta S^{\ddagger} = (-34 \pm 1)$ cal mol^{-1} K^{-1}. For the reaction of $[\mathbf{2}^{tBu2}]^+$ with benzyl alcohol, rate data were collected over ranges of substrate concentration and temperature. The Eyring plot of $\ln(k_1K/T)$ versus $1/T$ is linear and when fit gives values of $\Delta H^{\ddagger} = (11.1 \pm 0.8)$ kcal mol^{-1} and $\Delta S^{\ddagger} = (-29 \pm 3)$ cal mol^{-1} K^{-1} for the overall sequence of substrate binding and H-atom abstraction. Though the values of K alone are more scattered, the van't Hoff plot of $\ln(K)$ versus $1/T$ can be fit linearly to determine $\Delta H^{\circ} = (-3.2 \pm 0.6)$ kcal mol^{-1} and $\Delta S^{\circ} = (-9 \pm 2)$ cal mol^{-1} K^{-1}. The negative entropy for the equilibrium is consistent with an association of $[\mathbf{2}^{tBu2}]^+$ with substrate. Deduction of ΔH° and ΔS° (determined from K) from the overall values of $\Delta H^{\ddagger}$ and $\Delta S^{\ddagger}$ (determined from k_1K) determines the activation parameters of the actual rate-determining step (k_1) to be $\Delta H^{\ddagger\prime} = 14.3 \pm 1.0$ kcal mol^{-1} and $\Delta S^{\ddagger\prime} = 21 \pm 3$ cal mol^{-1} K^{-1}. These data are summarized in Table 1.

Large KIEs such as those seen for the $[\mathbf{1}^{tBu2}]^+$/benzyl alcohol reaction are often attributed to quantum tunneling. This phenomenon can be positively identified by an unusually small ratio of the Arrhenius preexponential factors for H- versus D-abstraction (A_H/A_D), less than the classical minimum of ∼0.7.[26] Because of the slow reaction rates and large KIE at the upper temperature limit of the reaction mixture (the boiling point of CH_2Cl_2 is 313 K), direct measurement of rate data for α-benzyl-d_2 alcohol over a range of temperatures is impractical. Instead, rate data were computed from the intramolecular KIE and the known absolute rates with benzyl-h_2 alcohol (k_2(H), Table 2) over the temperature range 268−308 K; assuming that the secondary KIE of the intramolecular experiment is near unity, $k_2(D) = k_2(H)/KIE_{intra}$. Linear plots of $\ln(k_2(H))$ and $\ln(k_2(D))$ versus $1/T$ (Figure 5) were fitted to obtain Arrhenius factors of $\ln(A_H) = 11.4$ and $\ln(A_D) = 11.2$; these values give an unexceptional ratio of $A_H/A_D = 1.2$.

(c) Reaction with 9,10-Dihydroanthracene. Because $[\mathbf{1}^{tBu2}]^+$ and $[\mathbf{2}^{tBu2}]^+$ react with benzyl alcohol by different mechanisms, it is not possible to directly compare the efficacy of their reactivity. To attempt such a comparison, their reactions with the benchmark hydrogen-atom abstraction substrate 9,10-dihydroanthracene (DHAn) were also studied.

Addition of DHAn to solutions of $[\mathbf{1}^{tBu2}]^+$ or $[\mathbf{2}^{tBu2}]^+$ causes their intense colors to fade. GC analysis of the final solution finds that anthracene (An) is produced in less than or equal to a 50% yield relative to the initial amount of oxidizing complex, confirming a 2:1 oxidant-to-substrate ratio. Trace amounts of anthraquinone are also observed, even when the reactions were conducted in putatively dioxygen-free conditions. The optical spectra of the final solutions contain the absorptions of the protonated, copper(II)-containing $[\mathbf{1}H]^+$and $[\mathbf{2}H]^+$. Therefore, similarly to benzyl alcohol, the overall reaction is

$$2[Cu^{II}L^{\bullet}]^+ + DHAn \rightarrow 2\,[Cu^{II}LH]^+ + An$$

Optical monitoring of the visible features of $[\mathbf{1}^{tBu2}]^+$ and $[\mathbf{2}^{tBu2}]^+$ during their respective reactions with DHAn show that their decay can be well-fit as pseudo-first-order processes. For $[\mathbf{2}^{tBu2}]^+$, k_{obs} is linear with DHAn concentration over the range 0.010−0.50 M, leading to an overall second-

(26) Kwart, H. *Acc. Chem. Res.* **1982**, *15*, 401−408.

Table 1. Kinetic and Thermodynamic Parameters for Reactions of $[\mathbf{1}^{tBu2}]^+$ and $[\mathbf{2}^{tBu2}]^+$ with BA and DHAn

reacn	const	$\Delta H^{\ddagger}$ (kcal mol^{-1})	$\Delta S^{\ddagger}$ (cal mol^{-1} K^{-1})	$\Delta H°$ (kcal mol^{-1})	$\Delta S°$ (cal mol^{-1} K^{-1})
$[\mathbf{1}^{tBu2}]^+$/BA	k_2	11.1 ± 0.4	−34 ± 1		
$[\mathbf{2}^{tBu2}]^+$/BA	k_1K	11.1 ± 0.8	−29 ± 3		
	K			−3.2 ± 0.6	−9 ± 2
	k_1[a]	14.3 ± 1.0	21 ± 3		
$[\mathbf{1}^{tBu2}]^+$/DHAn	k_1K	n/a	n/a		
$[\mathbf{2}^{tBu2}]^+$/DHAn	k_2	9.3 ± 0.6	−31 ± 2		

[a] Extrapolated from data for k_1K and K.

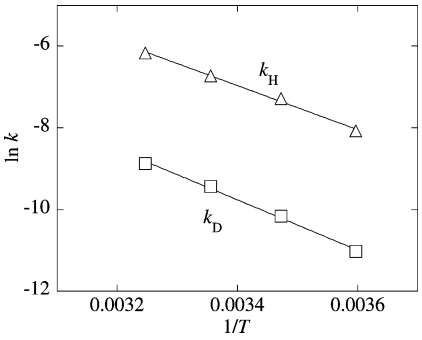

Figure 5. Arrhenius plots of the temperature dependence of the rate constants for α-*h*-abstraction versus α-*d*-abstraction of benzyl alcohol by $[\mathbf{1}^{tBu2}]^+$. Fit data for ln(k_H) vs 1/T: slope = −5400 ± 300 K; intercept = 11.4 ± 0.9. Fit data for ln(k_D) vs 1/T: slope = −6200 ± 300 K; intercept = 11.2 ± 0.9.

Table 2. Temperature Dependence of the Intramolecular Kinetic Isotope Effect for the Reaction of $[\mathbf{1}^{tBu2}]^+$ with α-*B*enzyl-d_1 Alcohol and Calculated Rate Constants for Deuterium Abstraction (k_D)

	temp (K)			
const	278	288	298	308
k_H (10^{-3} M^{-1} s^{-1})	0.31	0.69	1.2	2.1
k_H/k_D (KIE_{intra})	19	18	15	15
k_D (10^{-3} M^{-1} s^{-1})	0.016	0.038	0.084	0.14

order rate law with $k_2 = 0.13 \pm 0.01$ M^{-1} s^{-1} at 298 K (Table 3 and Figure 6). Unexpectedly, k_{obs} for the $[\mathbf{1}^{tBu2}]^+$/DHAn reaction is not linear over the same range but instead shows saturation behavior like that seen for the $[\mathbf{2}^{tBu2}]^+$/benzyl alcohol reaction. At 298 K, using eq 1, k_{obs} for the $[\mathbf{1}^{tBu2}]^+$/DHAn reaction can be fit well to give $k_1 = 0.37 \pm 0.03$ s^{-1} and $K = 1.1 \pm 0.1$ M^{-1}.

Reactions of $[\mathbf{1}^{tBu2}]^+$ and $[\mathbf{2}^{tBu2}]^+$ with isotope-labeled dihydroanthracene-9,9,10,10-d_4 (d_4-DHAn) gave k_{obs} values of $(1.73 \pm 0.03) \times 10^{-3}$ s^{-1} (0.050 M) and $(1.38 \pm 0.02) \times 10^{-3}$ s^{-1}, respectively, corresponding to KIEs of 16 and 5 for $[\mathbf{1}^{tBu2}]^+$ and $[\mathbf{2}^{tBu2}]^+$, respectively, at 298 K. C−H bond cleavage therefore is an important part of the rate-determining step in both cases, as was found for the benzyl alcohol reactions. The large, nonclassical KIE for the $[\mathbf{1}^{tBu2}]^+$/DHAn reaction is also comparable to the nonclassical KIE found for the $[\mathbf{1}^{tBu2}]^+$/benzyl alcohol reaction.

Variable-temperature studies aimed to extrapolate activation parameters for the reactions of $[\mathbf{1}^{tBu2}]^+$ and $[\mathbf{2}^{tBu2}]^+$ with DHAn were attempted to provide comparisons to their reactions with benzyl alcohol. For the $[\mathbf{2}^{tBu2}]^+$/DHAn reaction, Eyring analysis of k_2 over the temperature range 258−298 K (Table 4) provided $\Delta H^{\ddagger}$ and $\Delta S^{\ddagger}$ estimates of 9.3 ± 0.6 kcal mol^{-1} and −31 ± 2 cal mol^{-1} K^{-1}. The kinetics of the $[\mathbf{1}^{tBu2}]^+$/DHAn reaction inexplicably deviate from first-order behavior at temperatures lower than 288 K (15 °C). As the upper limit of the reaction temperature is ∼35 °C due to the boiling point of the solvent, the available temperature range is too narrow to provide good estimates of the activation parameters for this reaction.

Discussion

The kinetic behavior of the reactions of the copper(II)−phenoxyl complexes $[\mathbf{1}^{tBu2}]^+$ and $[\mathbf{2}^{tBu2}]^+$ with benzyl alcohol or DHAn reveals two types of mechanism. In the first (Scheme 2), the rate-determining step is a simple bimolecular reaction between $[Cu^{II}L^{\bullet}]^+$ and substrate as observed for the $[\mathbf{1}^{tBu2}]^+$/benzyl alcohol and $[\mathbf{2}^{tBu2}]^+$/DHAn reactions. In the second (Scheme 3), a substrate-binding equilibrium precedes a unimolecular reaction as observed for the $[\mathbf{2}^{tBu2}]^+$/benzyl alcohol and $[\mathbf{1}^{tBu2}]^+$/DHAn reactions. Initially, it appeared possible that $[\mathbf{2}^{tBu2}]^+$/benzyl alcohol binding could involve a copper−alcohol(ate) interaction similar to that proposed for the mechanism of GOase. However, high concentrations of benzyl alcohol do not affect the $[\mathbf{2}^{tBu2}]^+$ chromophore (at 1.0 M benzyl alcohol, $K = 3$ implies that ∼75% of $[\mathbf{2}^{tBu2}]^+$ is bound to substrate), nor does 1-octanol have an inhibitory effect on the reaction. The subsequent discovery of saturation behavior in the $[\mathbf{1}^{tBu2}]^+$/DHAn reaction indicates that the substrate-binding interaction is not necessarily associated with the presence of a polar hydroxy group but may arise from either $\pi-\pi$ stacking or cation$-\pi$ interactions. It is also possible that the high concentrations of substrate in the experiments (up to ∼10% (w/v)) change the solvent properties and thereby affect the reaction rates. However, in each case the reaction rates of the copper(II)−phenoxyl complex not showing saturation behavior remain linear over the same substrate concentration range. Therefore, complex−substrate association is the more likely cause of the saturation effects.

The large kinetic isotope effects (k(H)/k(D)) for each of these reactions indicate that the rate-determining steps involve cleavage of the relevant C−H bonds. Comparison across three substrates offers more insight into this step: 1-octanol does not react at an appreciable rate to form 1-octanal, benzyl alcohol does react, though slowly, and DHAn reacts rapidly, ∼25−300 times faster than benzyl alcohol. A key difference between these substrates is the bond dissociation energy (BDE) of the relevant C−H bond, for the reaction rate increases as the BDE decreases (C−H BDEs in kcal mol^{-1}: 1-octanol, ∼93; benzyl alcohol, ∼88; DHAn, ∼76).[27] This relationship is only valid if the hydroxy

(27) Luo, Y. R. *Handbook of Bond Dissociation Energies in Organic Compounds*; CRC Press: Boca Raton, FL, 2003.

Table 3. Observed Rate Constants for Reactions of $[\mathbf{1}^{tBu2}]^+$ and $[\mathbf{2}^{tBu2}]^+$ (0.1 mM) with DHAn in CH_2Cl_2 at 298 K

		[DHAn] (mol L^{-1})					
		0.50	0.25	0.10	0.050	0.025	0.010
k_{obs} (10^{-1} s^{-1})	$[\mathbf{1}^{tBu2}]^+$	1.31	0.764	0.357		0.0969	
		1.24	0.764	0.358		0.0958	
	$[\mathbf{2}^{tBu2}]^+$	0.606		0.131	0.0709	0.0392	0.0201
		0.734		0.135	0.0729	0.0433	0.0250

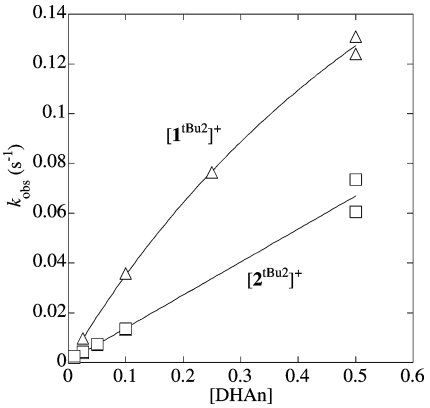

Figure 6. Plot of the pseudo-first-order rate constant k_{obs} versus DHAn concentration for the reactions of $[\mathbf{1}^{tBu2}]^+$ (triangles) and $[\mathbf{2}^{tBu2}]^+$ (squares) with DHAn in CH_2Cl_2 at 298 K. The data are shown with a fit derived from eq 1 for $[\mathbf{1}^{tBu2}]^+$ ($k_1 = 0.37 \pm 0.03$ s^{-1}, $K = 1.1 \pm 0.1$ M^{-1}) and a linear fit for $[\mathbf{2}^{tBu2}]^+$ (slope $= 0.13 \pm 0.01$ M^{-1} s^{-1}, intercept $= 0.001 \pm 0.001$ s^{-1}).

Table 4. Observed Rate Constants for Reaction of $[\mathbf{2}^{tBu2}]^+$ (0.1 mM) with DHAn (0.10 M) in CH_2Cl_2 at Variable Temperatures

	temp (K)				
	298	288	278	268	258
k_{obs} (10^{-2} s^{-1})	1.49	0.87	0.42	0.22	0.12
	1.49	0.95	0.45	0.22	0.11

Scheme 2

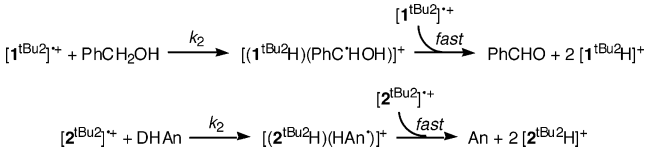

groups of the alcohols remain protonated, as deprotonation is estimated to lower the α-C−H BDE by 10−25 kcal mol^{-1}.[28] Due to the KIEs and BDE effect on rates, the rate-determining steps therefore are best described as homolytic cleavage of the C−H bond (i.e. hydrogen atom abstraction).[29] In this regard, the reaction mechanisms of the model complexes match that proposed for GOase, whose key substrate-oxidation step is best described as hydrogen atom abstraction.

The immediate products of hydrogen atom abstraction from either DHAn or benzyl alcohol would be the protonated, unoxidized form of the copper complex ($Cu^{II}L + H^+ = [Cu^{II}LH]^+$) and a highly reactive hydroanthracenyl ($HAn^{\bullet}$) or ketyl ($PhC^{\bullet}HOH$) radical. In the case of the DHAn reaction, the intermediacy of an $HAn^{\bullet}$ radical is supported by the trace amounts of anthraquinone observed in the reaction products that likely results from reaction with adventitious dioxygen.[30] However, because the hydrogen atom abstraction step is both rate-determining and product-determining as shown by the intermolecular and intramolecular KIE experiments with benzyl alcohol, the subsequent fast steps cannot be probed by absolute rate or product analysis. The denouement of the reaction mechanisms can therefore only be a subject of speculation. Two mechanisms by which the second 1 equiv of copper(II)−phenoxyl complex could complete the observed reaction are shown in Scheme 4; each has weaknesses. In steps analogous to the completion of the GOase oxidative half-reaction, the substrate-derived radical could further reduce the protonated copper(II) complex to copper(I) and transfer a second proton to generate An or PhCHO and $[Cu^{I}LH_2]^+$ (Scheme 4a). The diprotonated copper(I) complex would then rapidly comproportionate with $[Cu^{II}L^{\bullet}]^+$ to generate 2 equiv of $[Cu^{II}LH]^+$. However, the lack of a Cu^{II}/Cu^{I} reduction couple in the electrochemistry of both $\mathbf{1}^{tBu2}$ and $\mathbf{2}^{tBu2}$ speaks against this mechanism, albeit the potentials are not known for protonated or doubly protonated forms of these complexes. Alternatively, the substrate-derived radical could diffuse away and react directly with the second 1 equiv of $[Cu^{II}L^{\bullet}]^+$ to generate the final products (Scheme 4b). The presence of trace amounts of 1,4-anthraquinone in the products of DHAn oxidation is consistent with capture of intermediate $HAn^{\bullet}$ by dioxygen. However, the ketyl radical derived from benzyl alcohol should also be highly reactive with dioxygen, but even atmospheric levels of dioxygen do not affect the selectivity or yield in the benzyl alcohol oxidation reactions. The ultimate result from either sequence remains the same: each 1 equiv of $[Cu^{II}L^{\bullet}]^+$ is effectively only a one-electron oxidant.

Direct comparison of the reactivity of $[\mathbf{1}^{tBu2}]^+$ and $[\mathbf{2}^{tBu2}]^+$ is obfuscated because they react with each of the two substrates by different mechanisms. At low substrate concentrations where saturation is less evident, the reactions that include a substrate-binding equilibrium are faster in both cases: k_1K for the $[\mathbf{2}^{tBu2}]^+$/benzyl alcohol reaction is about 12 times k_2 for the $[\mathbf{1}^{tBu2}]^+$/benzyl alcohol reaction, and k_1K for the $[\mathbf{1}^{tBu2}]^+$/DHAn reaction is about 3 times k_2 for the

(28) Steigerwald, M. L.; Goddard, W. A.; Evans, D. A. *J. Am. Chem. Soc.* **1979**, *101*, 1994−1997.

(29) The ordering of the reaction rates could also correlate with the substrates' ionization energies and/or oxidation potentials, which should decrease with the increased aromaticity of benzyl alcohol or DHAn. However, an electron-transfer reaction pathway is unlikely due to the low redox potentials of $[\mathbf{1}^{tBu2}]^+$ and $[\mathbf{2}^{tBu2}]^+$ relative to those of the substrates, the parity of their reactivities despite differing in redox potential by 370 mV, and the large observed KIEs for these reactions.

(30) Bryant, J. R.; Taves, J. E.; Mayer, J. M. *Inorg. Chem.* **2002**, *41*, 2769−2776.

Scheme 3

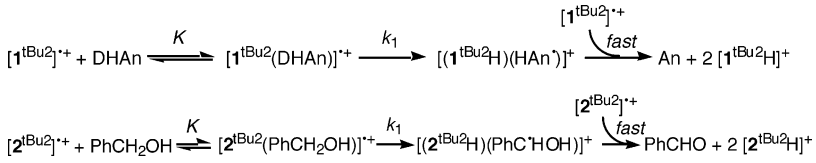

Scheme 4

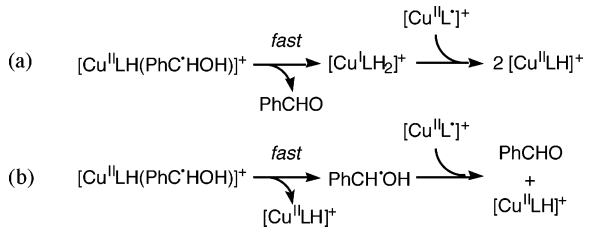

$[\mathbf{2}^{tBu2}]^+$/DHAn reaction. Presumably, the substrate-binding equilibria lower the entropic cost of the subsequent rate-determining steps and thereby accelerate the rates of the associative reactions. The determinations of activation parameters show that $\Delta S^{\ddagger}$ is indeed ~14 cal mol^{-1} K^{-1} lower for the $[\mathbf{2}^{tBu2}]^+$/benzyl alcohol reaction than for the $[\mathbf{1}^{tBu2}]^+$/benzyl alcohol reaction. If the entropic costs of the substrate-binding equilibrium and rate-determining step of the $[\mathbf{2}^{tBu2}]^+$/benzyl alcohol reaction are totaled (−29 cal mol^{-1} K^{-1}), the overall figure is still lower than for the $[\mathbf{1}^{tBu2}]^+$/benzyl alcohol reaction (−34 cal mol^{-1} K^{-1}). It was also hoped that comparison of $\Delta H^{\ddagger}$ for the reactions of $[\mathbf{1}^{tBu2}]^+$ and $[\mathbf{2}^{tBu2}]^+$ would provide insight into their relative inherent ability to abstract hydrogen atoms. $\Delta H^{\ddagger}$ for the $[\mathbf{1}^{tBu2}]^+$/benzyl alcohol reaction, 11 kcal mol^{-1}, is smaller than for the rate-determining step of the $[\mathbf{2}^{tBu2}]^+$/benzyl alcohol reaction (14 kcal mol^{-1}), though the overall enthalpic barrier of the latter reaction is only 11 kcal mol^{-1} when including the enthalpic effect of the substrate-binding equilibrium ($\Delta H^{\circ} = -3$ kcal mol^{-1}). Reversing the enthalpically favorable interaction of the substrate-binding step may be part of the rate-determining forward step. In that case, the remaining amount of 11 kcal mol^{-1} represents that proportion of the reaction barrier arising from C−H bond cleavage, putting the hydrogen atom abstraction ability of $[\mathbf{2}^{tBu2}]^+$ on par with that of $[\mathbf{1}^{tBu2}]^+$. That the rates of reaction of $[\mathbf{1}^{tBu2}]^+$ and $[\mathbf{2}^{tBu2}]^+$ with DHAn are similar despite the transfer of the advantage of a substrate-binding equilibrium, albeit weaker, to $[\mathbf{1}^{tBu2}]^+$ also indicates that the hydrogen atom abstraction abilities of the two copper(II)−phenoxyl species are comparable.

The activation energies and thus the rates for atom transfer reactions are expected to show some dependence on the thermodynamic driving force. At parity of substrate, this will be determined by the strength of the O(phenolate)−H bonds being formed in the $[\mathbf{1}^{tBu2}H]^+$ and $[\mathbf{2}^{tBu2}H]^+$ products.[31,32] The O−H bond dissociation energies for phenols in particular have been studied by treating proton and electron transfer as components of a thermodynamic cycle, such that relative BDEs could be approximated at 298 K by

$$\Delta\mathrm{BDE} = 1.37\Delta(\mathrm{p}K_a) + 23.06\Delta(E^{\circ}) \qquad (2)$$

where the pK_a values are of the relevant phenols and the E° values (in volts) are of the relevant phenolates.[33] Electron-withdrawing substituents such as carbonyl groups lower the pK_a value and increase E°, while electron-donating substituents such as alkyl groups raise the pK_a and decrease E°; of $\mathbf{1}^{tBu2}$ and $\mathbf{2}^{tBu2}$, $\mathbf{1}^{tBu2}$ has higher redox potentials and should have a lower pK_a due to the electron-withdrawing imine substituents on the phenolates. Following from the thermodynamic cycle summarized by eq 2, if $[\mathbf{1}^{tBu2}]^+$ and $[\mathbf{2}^{tBu2}]^+$ are considered to have the same affinity for hydrogen atom abstraction, it implies that the 370 mV lower oxidation potential of $\mathbf{2}^{tBu2}$ is compensated by an increase in its basicity by ca. 6 pK_a units. Exact pK_a values for $\mathbf{1}^{tBu2}$ and $\mathbf{2}^{tBu2}$ would be difficult to measure in CH_2Cl_2. The tabulated pK_a values of 4-acetylphenol and 4-methylphenol in DMSO are 14.0 and 18.9, respectively,[33] and their ΔpK_a value of 4.9 implies that a $\Delta(pK_a)$ value of 6 between $\mathbf{1}^{tBu2}$ and $\mathbf{2}^{tBu2}$ may be physically reasonable, though the differing polarities of DMSO and CH_2Cl_2 should affect the absolute pK_a values considerably.

The especially large KIEs in the reactions of $[\mathbf{1}^{tBu2}]^+$ with benzyl alcohol and DHAn deserve some comparison to the reactions of GOase itself and of other model complexes. The semiclassical limit for C−H/D isotope effects at room temperature is ~6−8; larger values are typically rationalized by invoking quantum tunneling.[26] The KIE of the substrate-oxidizing half-reaction of GOase with galactoside substrate is ~17 at room temperature, and a strong temperature dependence can be observed over the range of 4−45 °C that clearly indicates quantum tunneling effects;[34] in the reaction of GOase with substituted benzyl alcohols, KIEs are attenuated to values of 4−12 at room temperature.[6] GOase model complexes that react with external substrates have mostly shown H/D KIEs in the range of 5−8 at 298 K; a remarkable exception is the model complex $[Cu^{II}(L^4)]^+$ (Chart 2), which has extraordinary KIEs of ~50 and ~14 in its reactions with methanol and ethanol, respectively.[11] The reactions of $[\mathbf{1}^{tBu2}]^+$ and to a lesser extent $[\mathbf{2}^{tBu2}]^+$ therefore offered an unusual opportunity to positively identify quantum tunneling effects in a model complex like those seen for the native system. However, the variable-temperature study of the KIE of the $[\mathbf{1}^{tBu2}]^+$/benzyl alcohol reaction shows a classical A_H/A_D ratio near 1.0. An extended model comparing the reactivities of *h*- and *d*-labeled substrates in the tunneling regime has been proposed that predicts the coexistence of tunneling with

(31) Ingold, K. U.; Russell, G. A. In *Free Radicals*, 1 ed.; Kochi, J. K., Ed.; Wiley: New York, 1973; pp 283−293.
(32) Tedder, J. M. *Angew. Chem., Int. Ed. Engl.* **1982**, *21*, 401−410.
(33) Bordwell, F. G.; Cheng, J. P. *J. Am. Chem. Soc.* **1991**, *113*, 1736−1743.
(34) Whittaker, M. M.; Ballou, D. P.; Whittaker, J. W. *Biochemistry* **1998**, *37*, 8426−8436.

Chart 2

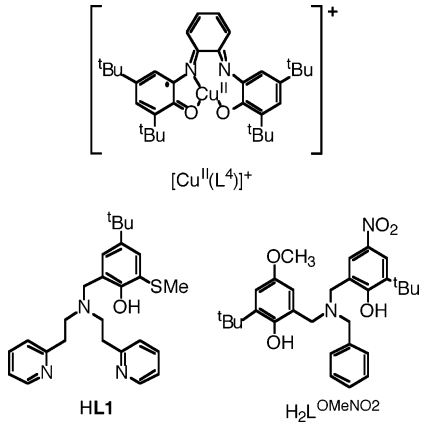

A_H/A_D values near unity at certain temperatures.[35] However, the limited temperature range of our experiments as bounded by solvent and reaction rate prevents confirmation of such behavior. An alternate explanation would be that a second isotope-dependent step with a KIE of 2−3 in combination with a primary KIE of 6−8 would amplify the overall reaction KIE to a value of 15−20, but no such second step is apparent in the reaction kinetics. Therefore, no definitive explanation for the high KIE value of the [**1**^{tBu2}]$^+$/benzyl alcohol reaction is left given the available data.

The single-turnover reactivity of [**1**^{tBu2}]$^+$ and [**2**^{tBu2}]$^+$ can be compared to the single-turnover reactivity of other model complexes, pictured in Chart 2 for reference. Reactions of [Cu^{II}(**L1**$^{\bullet}$)(NO$_3^-$)]$^+$ have been studied in some detail.[12,13] Its reactions with benzyl alcohol and 1,4-cyclohexadiene have overall second-order rate expressions linearly dependent on the concentrations of [Cu^{II}(**L1**$^{\bullet}$)(NO$_3^-$)]$^+$ and substrate. The k_2 values of 4.8×10^{-3} M^{-1} s^{-1} (benzyl alcohol) and 0.50 M^{-1} s^{-1} (1,4-cyclohexadiene) at 298 K in CH_3CN are similar to those determined for the reactions of [**1**^{tBu2}]$^+$ and [**2**^{tBu2}]$^+$. The activation parameters of the 1,4-cyclohexadiene reaction were found to be $\Delta H^{\ddagger} = 6.8$ kcal mol^{-1} and $\Delta S^{\ddagger} = -29$ cal mol^{-1} K^{-1}; the smaller value of $\Delta H^{\ddagger}$ relative to those for the [**1**^{tBu2}]$^+$ or [**2**^{tBu2}]$^+$/benzyl alcohol reactions reflects the smaller BDE of the 1,4-cyclohexadiene substrate (∼76 kcal mol^{-1}).[27] The complex [Cu^{II}(L^{OMeNO2}H)$^{\bullet}$(OAc)]$^+$ reacts with benzyl alcohol at a 10-fold faster rate ($k_2 = 2.7 \times 10^{-2}$ M^{-1} s^{-1} at 298 K in THF), but the reasons for this acceleration are not known.[15] Finally, the quinoidal copper complex [Cu^{II}(L^4)]$^+$ reacts with methanol and ethanol via a substrate-binding mechanism like that for the [**2**^{tBu2}]$^+$/benzyl alcohol reaction.[11] The rate constants for the rate-determining steps are low in comparison ($k_1 = 1.2 \times 10^{-5}$ s^{-1} and 2.0×10^{-5} for methanol and ethanol, respectively, at 298 K in CH_2Cl_2), but these substrates have much stronger C−H bonds. An important difference between the reactions of [Cu^{II}(**L1**$^{\bullet}$)(NO$_3^-$)]$^+$ and [Cu^{II}(L^{OMeNO2}H)$^{\bullet}$(OAc)]$^+$ with alcohols and those of [**1**^{tBu2}]$^+$ and [**2**^{tBu2}]$^+$ is that the tripodal complexes react with substrates in a 1:1 ratio, using the oxidizing equivalents of both the phenoxyl and the copper(II), while the latter salen-derived complexes react in only a 2:1 ratio, ultimately using only the oxidizing equivalent of the phenoxyl. The tripodal ligands may offer greater flexibility of coordination about copper and thereby better accommodate the geometrical preferences of copper(I), whereas the square-planar geometry of the ligands in [**1**^{tBu2}]$^+$ and [**2**^{tBu2}]$^+$ preferentially stabilizes copper(II). Additionally, the reaction conditions for the tripodal systems typically include acetonitrile as the solvent, whose coordination to copper can favor reduction to a copper(I) state.[36,37]

Beyond their inability to perform two-electron oxidation of substrates, [**1**^{tBu2}]$^+$ and [**2**^{tBu2}]$^+$ are deficient in matching the rate of reaction of GOase. While $\Delta G^{\ddagger}$ for the reactions of the model complexes with benzyl alcohol is ∼20 kcal mol^{-1} at 298 K, $\Delta G^{\ddagger}$ for the substrate-oxidizing half-reaction of GOase is estimated to be 11−14 kcal mol^{-1}, representing a rate at least 10^4-fold faster than those of the model systems even with inactivated substrates.[4,5] The acceleration due to substrate binding seen in comparisons of [**1**^{tBu2}]$^+$ and [**2**^{tBu2}]$^+$ is likely amplified by orders of magnitude in GOase. Modeling studies predict that the residues surrounding the GOase active site provide an extensive hydrogen-bonding network for enzyme-bound galactoside substrates, favoring the substrate-binding equilibrium, and furthermore specifically predispose the α-hydrogen atom of the primary alcohol for abstraction by the oxygen atom of the equatorial tyrosine radical.[38] Such specific interactions cannot be expected for simple complexes such as [**1**^{tBu2}]$^+$ and [**2**^{tBu2}]$^+$. Additionally, the axial tyrosine residue of the GOase active site is believed to deprotonate the alcoholic substrate, which should significantly lower the BDE of the α-C−H bond and favor hydrogen atom abstraction.[4] [**1**^{tBu2}]$^+$ and [**2**^{tBu2}]$^+$ do not incorporate such an internal base, and the relatively fast reaction rates of [**1**^{tBu2}]$^+$ or [**2**^{tBu2}]$^+$ with DHAn relative to the rates with benzyl alcohol argue against deprotonation of the alcoholic substrate prior to hydrogen atom abstraction. Rational incorporation of features such as substrate binding sites or internal bases into model complexes to accelerate reactivity is beyond the minimalist design of **1**^{tBu2} and **2**^{tBu2} but may ultimately be addressed by the use of supramolecular interactions in more sophisticated systems.[16]

Acknowledgment. This work was supported by the National Institute of Health (Grant GM50730 to T.D.P.S.). R.C.P. has been supported by an Urbanek Family Stanford Graduate Fellowship.

Supporting Information Available: Observed first-order rate constants and derived constants for the reaction of [**1**^{tBu2}]$^+$ and [**2**^{tBu2}]$^+$ with benzyl alcohol. This material is available free of charge via the Internet at http://pubs.acs.org.

IC048695I

(35) Jonsson, T.; Glickman, M. H.; Sun, S. J.; Klinman, J. P. *J. Am. Chem. Soc.* **1996**, *118*, 10319−10320.

(36) Kolthoff, I. M.; Coetzee, J. F. *J. Am. Chem. Soc.* **1957**, *79*, 1852−1858.

(37) Hathaway, B. J. In *Comprehensive Coordination Chemistry*; Wilkinson, G., Gillard, R. D., McCleverty, J. A., Eds.; Pergamon: Oxford, U.K., 1987; Vol. 5, pp 533−594.

(38) Wachter, R. M.; Branchaud, B. P. *J. Am. Chem. Soc.* **1996**, *118*, 2782−2789.